PHYSICAL REVIEW B **81**, 165401 (2010)

Plasmonic blackbody: Strong absorption of light by metal nanoparticles embedded in a dielectric matrix

V. G. Kravets, S. Neubeck, and A. N. Grigorenko
School of Physics and Astronomy, University of Manchester, Manchester M13 9PL, United Kingdom

A. F. Kravets
Institute of Magnetism, National Academy of Sciences of Ukraine, 36-b Vernadsky Boulevard, Kiev 03142, Ukraine
(Received 5 January 2010; revised manuscript received 7 March 2010; published 1 April 2010)

We have experimentally and theoretically demonstrated strong absorption of visible light in a thin nanostructured layer consisting of silver nanoparticles embedded in a dielectric matrix. Light absorption at the level of above 90% is recorded over a wide optical wavelength range (240–850 nm) and for a broad range of angles of light incidence (0°–70°) in extremely thin films (160 nm). We suggest a generic principle for enhancement of light absorption in thin layers of artificial metamaterials and show that effective refractive indices of our samples measured with the help of ellipsometry can be adequately described by an effective-medium theory. We demonstrate that a substantial fraction of light can be trapped in the nanostructured film due to scattering by noble metal nanoparticles and total internal reflection.

DOI: 10.1103/PhysRevB.81.165401 PACS number(s): 78.67.−n, 71.45.Gm, 73.22.Lp, 78.20.Ci

I. INTRODUCTION

An ideal blackbody is an object that absorbs all light that falls on it. Being a perfect absorber, a blackbody could be valuable for many important applications, e.g., photodetection or collection of solar energy (photovoltaic cells). Of particular interest are thin black body films which could efficiently trap photons and transfer their energy into electric or thermal energy. Such thin films are extremely difficult to find because there do not exist many natural materials that could absorb light over a wide optical wavelength range and for a broad range of angles of incidence and be integrated with silicon technology. A possible route to produce thin film absorbing coatings is to use plasmonic photonic crystal structures,[1,2] periodic metallic structures,[3–7] in which desired absorption is achieved via collective electronic excitations called plasmons, both propagating and localized. However, the resonant nature of these effects implies that absorption can only be large over a relatively narrow range of wavelengths. For example, Popov *et al.*[8] presented two-dimensional crossed gratings for total absorption of unpolarized light where high absorption was limited to small ranges of angles of incidence due to the sharply resonant nature of plasmon-polariton wave excitation. A strong absorption in a wide angular interval but in a small spectral interval has been demonstrated in shallow lamellar metallic gratings.[9]

In our recent work[10] we suggested a generic design for blackbodylike thin coatings and demonstrated its validity by producing nanostructured gold films about 100 nm thick that absorb visible light in a wide spectral range over a large range of incident angles. By analyzing Fresnel coefficients we showed that for any fixed thickness of a film, h, there exists a range of complex indices of refraction, n, of the layer placed on top of a substrate which would guarantee maximal light absorption.[10] The values of the refractive indices that would yield the strongest absorption for the nanofilms are not readily available in natural materials. We have shown, however, that suitably nanostructured metal-dielectric composites could possess the desired effective refractive indices. To describe optical behavior of our structures we used the Maxwell-Garnett effective approach[11,12] and showed that the gold stripes can be considered as a homogeneous layer with an effective refractive index that would guarantee very strong absorption of visible light in the system. Our experimental structures[10] were made by electron beam lithography which is expensive. A development of thin inexpensive absorbing coatings would greatly increase their area of applications. Feasible low-cost techniques could be based on silicon nanostructures which can be grown from the gas phases (physical-vapor deposition methods) or chemical catalyzing methods. The absorbing layer for solar cells should ideally be thin (~100 nm) with the absorption above 90% in the range of wavelengths 400–900 nm where the sun spectral intensities achieve maximal values.

The main aim of this paper is to demonstrate blackbody-like coatings working in wide spectral region [visible-near infrared (IR)] and broad angles interval (up to 70°) produced by an inexpensive evaporation technique. In this paper we present results for nanostructured films made of a mixture of Ag particles in Al_2O_3 matrix. Silver has a very small imaginary part of the dielectric constant and very high electrical conductivity, which leads to the excellent optical and electronic properties of silver nanostructures. These excellent properties have motivated us to study silver nanoparticles embedded in a dielectric matrix with the aim to achieve strong light absorption in a broad spectral region. In addition to it, Ag, due to its lower absorption and lower cost is thus better choice than Au, although it should be well encapsulated to avoid oxidation effects that are not present for Au. We chose Al_2O_3 as a dielectric layer because of its very stable chemical behavior and high refractive index ~1.7. We demonstrate that extremely high absorption (~95%) could be achieved with 100–120 nm Ag particles randomly distributed in Al_2O_3 with volume concentration about 15%. It should be stressed that manufacturing of such type of high absorber devices does not require expensive lithographic

(optical or electron beam) techniques and can be optimized for production of large sizes of low-cost solar cells. These structures permit a high level of absorption (more than 90%) of unpolarized light in a wide range of incident angles (−45°,+45°). Absorption higher than 95% for *p*-polarized light is revealed over a range of angles of incidence (−70°,+70°).

The paper is organized as follows. Section I provides the description of experimental methods and procedures. We discuss the results obtained on the fabricated samples in Sec. II. In Sec. III we discuss the theory of a plasmonic blackbody based on artificial films produced by inclusion of metallic nanoparticles into a dielectric host. We provide the analytical formula for the silver dielectric constants derived from the spectroscopic ellipsometry measurements and present the results of the calculations based on the Maxwell-Garnett theory. We compare the experimental results with theory in Sec. IV. Finally, the conclusion is given.

II. EXPERIMENTAL PROCEDURES

The $Ag_x(Al_2O_3)_{1-x}$ nanostructured films (where $x=0.07–0.9$ is the atomic fraction of Ag) of large areas (2.5×2.5 cm^2) of thickness ~150–160 nm were deposited using e-beam evaporation from Ag and Al_2O_3 independent sources onto glass substrates. The pressure was less than 10^{-4} Pa during the film deposition. The composition of the films was determined using energy-dispersive x-ray analysis. The crystalline structure was investigated by x-ray diffraction and scanning electron microscopy (SEM). The fabrication conditions were adjusted to achieve an average particle diameter $D\sim100–120$ nm with an average interparticle separation distance larger than the particle diameters ($0.08<f<0.3$, f is the volume fraction of Ag particles). The thickness of deposited films has been chosen slightly higher than the average diameter of the silver spheres.

The ellipsometric measurements were performed with a Woollam VASE variable angle ellipsometer of rotating-analyzer type in the wavelengths range of 240–1000 nm. The complex dielectric function $\varepsilon(\lambda)=\varepsilon_1(\lambda)+i\varepsilon_2(\lambda)$ was directly determined from ellipsometric parameters $\psi(\lambda)$ and $\Delta(\lambda)$.[13] The inversion of ellipsometric data was performed within the framework of film-substrate model (pure substrate was also measured). We take into account possible perturbations of the ellipsometric data due to surface roughness or grain texturing. Our measurements at multiple angles of incidence from 45° to 80° confirm that the surface roughness effect on $\varepsilon(\lambda)$ is less than 2–5 % over the measured spectral range and therefore does not significantly influence relative changes in $\varepsilon(\lambda)$. From atomic force microscopy images the rms value of the surface roughness was found to be less than ~10 nm.

We have also measured reflection and transmission for *p*- and *s*-polarized light for angles of incidence of light 0°–80° using Ocean Optics USB2000 spectrometer. The spectrometer is equipped with a xenon light source. The light passed through a polarizer and then was focused by objective on the surface of the sample to a spot of approximately 200 μm. The sample was mounted on a rotation stage. The transmitted light was collected using an optical fiber coupled to the spectrometer (200 μm core). The transmission spectra were found by normalizing spectra measured through the sample with respect to the spectra measured through the air.

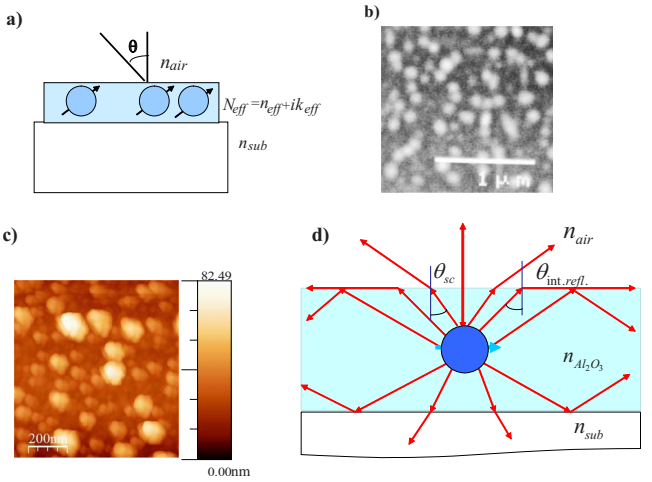

FIG. 1. (Color online) Schematics of perfect absorber blackbody. (a) Schematic view of the nanostructured layer on a substrate. (b) A SEM image of one of the studied silver nanostructures. (c) AFM image of silver nanostructures with volume filling factor of Ag, $f=0.15$. (d) Schematic illustration of the light trapping in nanostructured film due to dipole scattering on a nanoparticle.

III. EXPERIMENTAL RESULTS

Metal films are usually highly reflective in the visible and infrared regions even at small thicknesses. Indeed, light waves are evanescent inside metals and penetrated at small distance in metallic films (the skin depth). Using the measured refractive index for pure Ag film[14] we can estimate skin depth as $\lambda/(4\pi k)$, which is about 13 nm in the visible and near IR region. If the thickness of an Ag film is much larger than the skin depth, transmission can be neglected and most of light is reflected. The reflectivity of bulk silver is almost independent of wavelength and close to 100% over the entire visible region.[14] Consequently, the absorption of plain Ag layers is usually small. For example, 100-nm-thick plain Ag film absorbs only about 3–4 % in the visible region and about 2–3 % in the near IR region. It comes, therefore, as a nice surprise that a composite material made from Ag nanoparticles embedded into a dielectric layer can demonstrate extremely high level of absorption as described in the experiments and theory below.

Silver nanoparticles of varying volume filling fractions, f, were deposited into Al_2O_3 amorphous matrix. SEM image, Fig. 1(b), shows a typical morphology of these films. Particle sizes and the filling fraction were controlled by the deposition ratio of Ag and Al_2O_3. Film thickness was determined from ellipsometry and profilometry and ranged from 150 to 160 nm. The structural characterization was also done by atomic force microscopy (AFM). AFM analysis is performed in the tapping mode on the sample to examine the surface morphology in a scan area of 1.0×1.0 μm^2. AFM image of the Ag-Al_2O_3 nanostructure is shown in Fig. 1(c). AFM im-

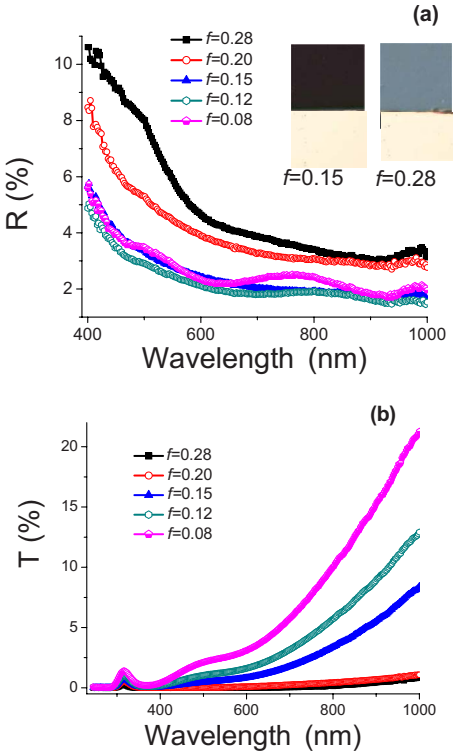

FIG. 2. (Color online) Optical properties of the Ag-Al_2O_3 nanostructures for different filling factor of Ag, $0.08 \leq f \leq 0.28$. (a) The reflection spectra for the light of p polarization at normal incidence and (b) the transmission spectra for p-polarized light at normal incidence. Insets show the polarization-contrast optical microscopy images for reflected light for two samples: $f=0.15$ and $f=0.28$.

age demonstrates the presence of a large number of Ag nanoparticles in films. The average particle diameter was between 80 and 120 nm (about 100 nm in the composite with $f \approx 15\%$).

We measured reflection and transmission coefficients for Ag-Al_2O_3 nanostructures with different volume concentration of Ag. Figure 2 shows the corresponding reflectance and transmittance spectra of nanocrystalline Ag-Al_2O_3 films at normal incidence. The reflected intensity (Fig. 2) is expectedly high ($\sim 5-10$ %) at $\lambda \sim 400$ nm; it then falls monotonously below $\lambda \sim 450$ nm and reaches approximately constant values $\sim 2-3$ % for wide spectral range 500–1000 nm. Note that with a decrease in the volume concentration of Ag nanoparticles the reflectance decreases at all wavelengths. As we can see from Fig. 2, the fabricated nanocomposite layer behaves like bulk silver for large volume concentration of Ag ($f \sim 0.3$) resulting in no transmission. The transmission peaks at around 320 nm are connected to plasmon resonances of silver nanoparticles. The transmission of less than 3% is observed for wide spectral region 250–800 nm for concentration of Ag nanoparticles of about 15 vol %. It is worth noting that with increasing of volume concentration of Ag the particle size slightly increases.

Our measurements reveal that the smallest value of $R(\lambda)$ and $T(\lambda)$ is very sensitive to the volume concentration of Ag nanoparticles. Thus we conclude that the changes in concentration of Ag particles embedded in Al_2O_3 matrix (and their sizes) strongly affect the enhancement of absorption. We found that the optimal geometrical parameters for the design of blackbodylike nanostructures are as follows: volume filling factor $f \approx 0.15$, diameter of silver particular $D \approx 100-120$ nm, and thickness of layer $h \approx 160$ nm. More importantly, it was found that the reflection and transmission can show low values in a large wavelength range ($\leq 2\%$ for some angles of incidence). Note that the absorption can be approximately enhanced by 2 orders of magnitude over bulk Ag.

To further investigate enhancement of absorption for the studied metamaterials, we recorded the reflection and transmission at different angles of light incidence. Measurements of optical transmittance, $T(\lambda)$, and reflectance, $R(\lambda)$, were made over the spectral range 250–1000 nm at angles of incidence, θ, from 0° to 70° for both incident p- and s-polarized radiations. The results are shown in Figs. 3(a) and 3(b) and the most important features of these curves are as follows. For incident angles up to 65° the reflectivity is close to 2% for p-polarized light at the wavelength range of 240–1000 nm. For these angles of incidence we observed pronounced reflectivity plateau with values of $R_p(\lambda)$ as low as 2% in the spectral range 400–1000 nm. More detailed analysis shows that for p-polarized light angular dependence of spectra $R_p(\lambda)$ exhibits maximum in the range $\lambda \sim 350-370$ nm for $\theta \geq 60°$ and then decrease with increasing the incident wavelength. This peak becomes increasingly prominent with increasing incident angle.

Figure 3(b) shows the transmission spectra of the studied nanostructures for p-polarized light, for the incident angles $\theta = 0°-70°$. They show an increase in the intensity of transmitted light with increasing wavelength. The spectra for different angles of incidence, θ, are similar. The optical transmission for p-polarized light leads to a low value less than 3% for a wavelength range of 240–850 nm. For angles of incidence $\theta \geq 60°$ the level of intensity for the transmitted light in the whole spectral range of 240–1000 nm is close to 1–2 %. We see that the changes in the intensity of transmitted light for investigated spectral region are negligible. Note that the value of transmitted intensity for low wavelengths is close to zero, except near $\lambda \sim 320$ nm where it is about 1%. In Fig. 3(c) we see that the absorption rises to the relatively large value more than 95% for wide spectral region 400–850 nm and angles of incidence from 0° to 70°. This result confirms that the absorption of light is very high and is rather insensitive to angles of incidence due to spherical symmetry of the silver nanoparticles. This enhanced absorption occurs for p-polarized light in a range of angle of incidence equal (−70°:70°).

In contrast to the p-polarization results, the s-polarization reflectivity shows an increase in intensity from 7% to 47% [Fig. 4(a)] with increasing incident angle. At low angles, $\theta \leq 45°$, the reflectivity spectra for both polarizations are similar. This is due to the fact that the absorption for both polarizations at low incidence angles is generated by the electric-field component parallel to the film plane. At high incidence angles, the perpendicular to plane of incidence electrical-field component becomes much larger than the parallel one which affects reflection of p-polarization. Figure 4(b) shows the optical transmission spectra for the light of s-polarization

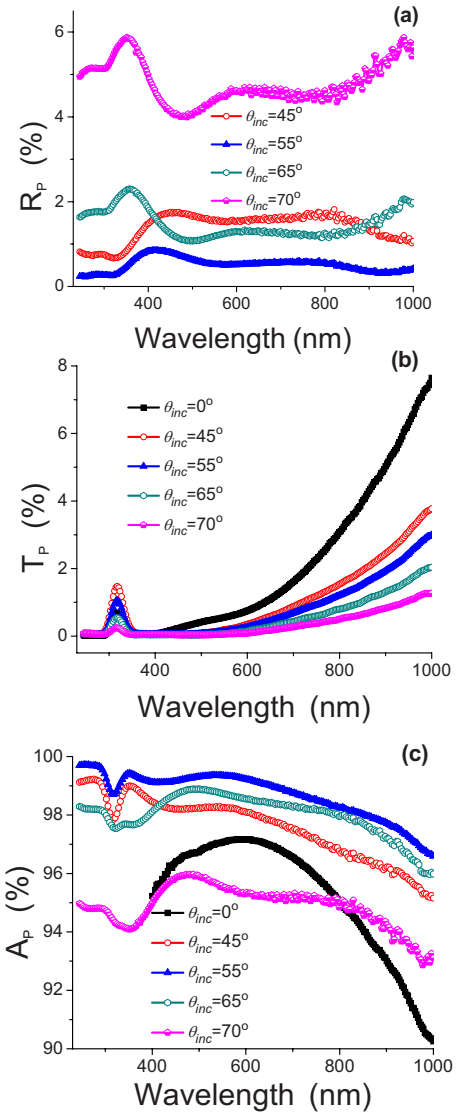

FIG. 3. (Color online) Optical properties of the Ag-Al_2O_3 nanostructures with $f=0.15$ and $D\approx 120$ nm. (a) The reflection spectra for the light of p polarization and $45°\leq\theta\leq 70°$. (b) The transmission spectra for the light of p polarization and $0°\leq\theta\leq 70°$. (c) The absorption spectra for the light of p polarization.

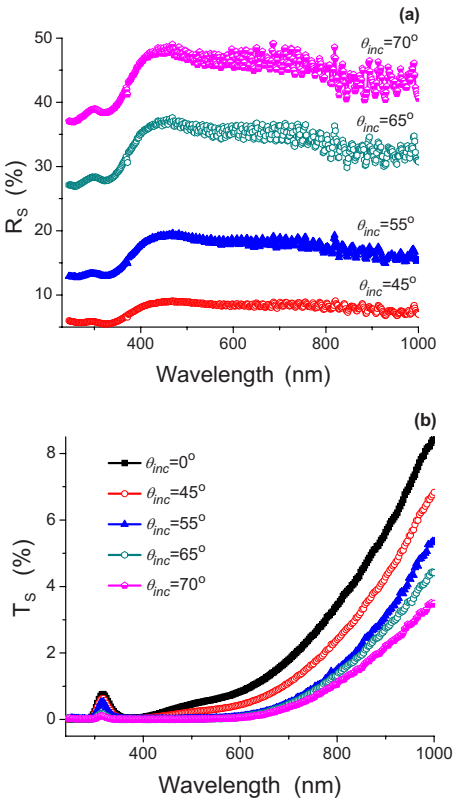

FIG. 4. (Color online) Optical properties of the Ag-Al_2O_3 nanostructures with $f=0.15$ and $D\approx 120$ nm. (a) The reflection spectra for the light of s polarization and $45°\leq\theta\leq 70°$. (b) The transmission spectra for the light of s polarization and $0°\leq\theta\leq 70°$.

and $0°\leq\theta\leq 70°$. We can see that the transmission spectra for both p- and s-polarizations [Figs. 3(b) and 4(b)] are similar only values of T_S are slightly higher than T_P for long wavelengths. Combining data shown in Figs. 3 and 4 we conclude that such metal nanostructures can strongly absorb light (more than 90%) of both p- and s-polarizations (or unpolarized light) in a wide range of incidence ($0°\leq\theta\leq 45°$).

As the average particle size of the embedded nanocrystalline silver into Al_2O_3 matrix is changed, we observe by eyes a marked change in its color, from white (in the bulk) to black for particles with sizes of 100–120 nm. Inset of Fig. 2(a) shows the polarization-contrast optical microscopy images for reflected light for two samples: $f=0.15$ and $f=0.28$. We see that the reflection from our sample ($f=0.15$) is very small for the p-polarized light. This picture confirms the blackness of our nanostructured film.

IV. THEORY

Let us consider a monolayer of metal nanoparticles embedded in oxide matrix and deposited onto a dielectric substrate as shown in Fig. 1(a). It is supposed that the spatial distribution of nanoparticles in the oxide matrix is random and the distances between particles are comparable with the wavelength of light. We are looking for a structure that could strongly increase light absorption (and hence improve efficiency of a solar cell or a photodetector). There are two basic ways how an enhancement of photocurrents due to the presence of covering layers can be achieved: (i) concentration of a scattered (diffracted) light into an absorbing (e.g., photoactive) region or (ii) near-field light concentration into an absorbing region. According to the Mie theory for a single spherical particle,[15] the relative strengths of light absorption and scattering can be determined from the absorption and scattering cross sections σ_{abs} and σ_{sca} of the individual particles,[15]

$$\sigma_{abs}=\frac{2\pi}{\lambda}\mathrm{Im}(\alpha), \tag{1a}$$

$$\sigma_{sca}=\frac{1}{6\pi}\left(\frac{2\pi}{\lambda}\right)^4|\alpha|^2. \tag{1b}$$

Here, α is the polarizability of the particle and λ is the wavelength. We define the scattering efficiency Q_{rad} of the par-

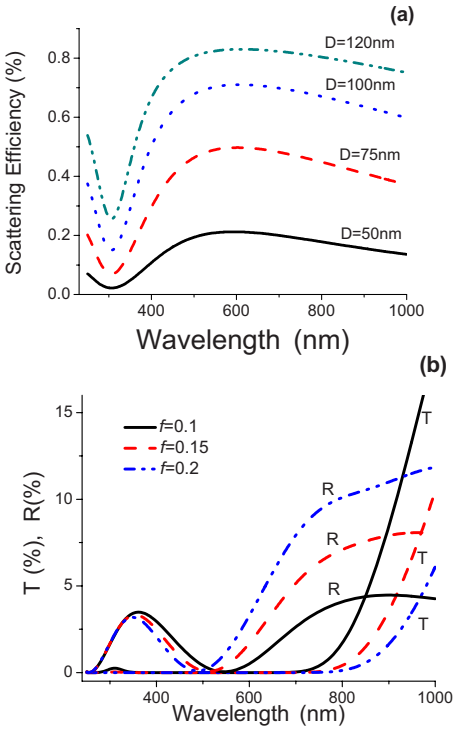

FIG. 5. (Color online) (a) Scattering efficiency for the Ag-Al_2O_3 nanostructures as a function of particle diameter, D; (b) the numerical results for transmission and reflection spectra at normal incidence for the Ag-Al_2O_3 nanostructures with different volume fraction of Ag: $f=0.1, 0.15, 0.2$.

ticles as $Q_{rad}=\sigma_{sca}/(\sigma_{sca}+\sigma_{abs})$. Note that Q_{rad} represents the fraction of the extinction energy that is reradiated.

Figure 5(a) shows a plot of Q_{rad} as a function of the particle diameter, D. The scattering efficiency Q_{rad} increases as the particle size is increased. This occurs because larger particles have higher polarizabilities, resulting in larger radiative losses. The sharp drop in Q_{rad} at short wavelengths is due to interband transitions in silver particles. Note that the size of particles cannot be increased indefinitely because the particles should be much smaller than the wavelength of light. Figure 5(a) demonstrates that scattering efficiency more than 80% can be achieved for Ag nanoparticles embedded into Al_2O_3 with diameters about 120 nm. For dense particle arrays, the light scattered by nanoparticles is responsible for reflected or refracted rays due to light interference. However, in our case of a sparse array of nanoparticles embedded into a dielectric matrix (with particle separation comparable with the light wavelength) the light scattered by nanoparticles could be effectively trapped in the dielectric layer due to the total internal reflection, see Fig. 1(d), and be eventually absorbed. It is easy to evaluate the trapping angle of light as $\arcsin(1/n)=35°$ for the normal light incidence at the air-film interface. This implies that only radiation going into the top 1.2 sr [which is about $1.2/(4\pi)\approx 9\%$ of the total solid angle] will partially escape the film into the air. There exists an optimum combination of the particle diameter, D, and their filling fraction, f, in dielectric matrix (with high real refractive index, n) that maximizes the light trapping and optical absorption based on such structures.

We can therefore associate attenuation of a light coming through our samples with scattering and absorption. The extinction cross section is therefore the sum of the scattering and absorption cross sections: $\sigma_{ext}=\sigma_{sca}+\sigma_{abs}$. Applying Lambert-Beer's law the resulting intensity transmitted through a monolayer of the noninteracting metal particles is: $T\propto\exp(-N\sigma_{ext}h_{eff})$ (where the particle number density, $N=\frac{3f}{4\pi a^3}$, is related to the filling factor f and the particle radius a; h_{eff} is the effective thickness of particle layer and its magnitude is larger than geometrical thickness of layer, h). In our simulation we set $h_{eff}\approx 10\lambda$ (λ is the wavelength). This value is consistent with the average path length of a trapped beam for Lambertian surfaces estimated by Yablonovitch (Ref. 16). Figure 5(b) shows the calculated transmission spectra versus wavelength for silver particles in Al_2O_3 matrix for low filling factor, f, ranging from 0.1 to 0.2. It can be seen that the decrease in the filling factor f gives rise to the transmission T for the large wavelengths. Note that the intensity of transmission spectra drops below 5% in the spectral region $\lambda=800$–900 nm, which is important due to light trapping at wavelength near the band gap of Si, commonly used in solar cells.

It is necessary to stress that a studied metamaterial is in the borderline between the effective medium and a random array of individual scatters. This leads to interesting and rich physics that includes light localization, random hot spots of absorptions, etc. At the same time, it makes extremely difficult for one to model all properties of the material with just one model. As an alternative to the theoretical model described above, we consider an effective medium approach to fabricated samples modified by the presence of trapped light modes. In our previous work (Ref. 10), using Fresnel coefficients for transmission and reflection coefficients we have shown that a thin film (of thickness ~ 100 nm) with the effective refractive index $n_{eff}\approx 1.2$–1.7 and $k_{eff}\approx 0.3$–0.6 in the visible and near IR region guarantees the maximal absorption of incident light. We show here that the studied arrays of Ag particles in the dielectric matrix also possess analogous optical constants.

To calculate the effective refractive index of the studied nanocomposites we use the Maxwell-Garnet effective-medium approximation (EMA).[11,12] EMA describes the interaction between the incident light and nanostructured materials and assigns a complex effective index of refraction to such structures. This approach worked surprisingly well being applied to plasmonic blackbody nanostructures based on gold nanostripes.[10] Here, the size of Ag particles is not small as compared to the wavelength of ultraviolet and visible light, and it becomes important to take into account the effects of multiple scattering in the optical response of the film structures. In this range of particle sizes the scattering effects are described with the help of the Mie theory of scattering.[15] In the dipole approximation of Mie's theory each nanoparticle can be represented by an electric dipole, $\boldsymbol{p}$, with the dipole polarizability α. For particles sizes $D\approx 100$ nm with non-negligible absorption loss in the approximation introduced by Doyle,[17] a dynamic polarizability can be written as,[15,17]

$$\alpha = i\frac{3a^3}{2x^3}a_1, \tag{2}$$

where $x=2\pi n_d a/\lambda$ is the size parameter ($n_d=\sqrt{\varepsilon_d}$ is the refractive index of Al_2O_3, $a=D/2$ is the radius of the particle). The Mie coefficient a_1 is given by[15,17,18]

$$a_1 = \frac{m\psi_1(mx)\psi_1'(x) - \psi_1(x)\psi_1'(mx)}{m\psi_1(mx)\xi_1'(x) - \xi_1(x)\psi_1'(mx)}, \tag{3}$$

where $\psi_1(x)$ and $\xi_1(x)$ are the Riccati-Bessel functions, $m=\sqrt{\varepsilon/\varepsilon_d}$ is the ratio of the index refraction of the silver spheres, ε, to that of the host dielectric (Al_2O_3).

This dipole approximation was shown to be adequate when distances between particles are on the order of or larger than their diameter D, i.e., for small volume fractions f ($f<0.5$). To calculate effective optical constants of a mixture, we follow the Maxwell-Garnet approach[11,12] and assume that the effective dielectric function of nanocomposite material is related to the dipole polarizability of nanoparticles by the Clausius-Mossoti equation,

$$\frac{\varepsilon_{eff}-\varepsilon_d}{\varepsilon_{eff}+2\varepsilon_d} = \frac{f}{a^3}\alpha. \tag{4}$$

This yields the following extended Maxwell-Garnett formula,[19]

$$\varepsilon_{eff} = \frac{a^3+2f\alpha}{a^3-f\alpha}\varepsilon_d. \tag{5}$$

To take into account the dispersion of the particle sizes (naturally arising during the deposition process), we introduce a size distribution function as a log-normal distribution,[17]

$$f_{LN}(D) = \frac{1}{(2\pi)^{1/2}\ln\sigma}\exp\left[-\frac{(\ln D/D_{av})^2}{2\ln^2\sigma}\right], \tag{6}$$

where D_{av} is the average diameter of the nanoparticles and σ is the standard deviation ($\sigma=1.5$, in our calculation). Then, the complex effective dielectric function, ε_{eff}, can be written as

$$\varepsilon_{eff} = \int_0^\infty \varepsilon_{eff}(D)f_{LN}(D)dD. \tag{7}$$

It is easy to see that the effective dielectric function, ε_{eff}, strongly depends on dielectric function of silver nanoparticles [see Eqs. (2)–(5)]. Permittivity of silver is the sum of the interband and intraband components and often depends on the way how silver was fabricated. In our calculations we assume that the permittivity of Ag nanoparticles of size ~100 nm is the same as that of a silver film of thickness ~100 nm. To find the optical constants, we have evaporated a thin silver film under the same conditions that were used in technology processes for preparing of Ag-Al_2O_3 mixtures. We have extracted the spectral dependences of the complex refractive index $n+ik=\sqrt{\varepsilon(\omega)}$ for the fabricated silver films using spectroscopic ellipsometry (performed with a Woollam spectroscopic ellipsometer). The extracted dielectric function, ε, was then modeled by fitting with two Lorentz functions and the Drude term,[10]

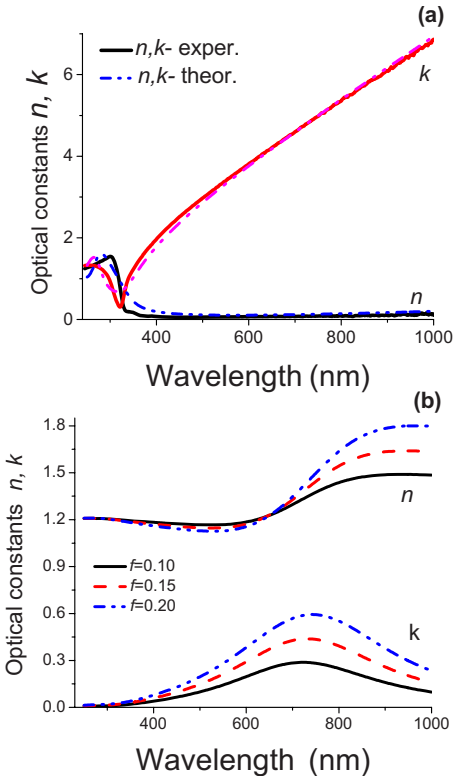

FIG. 6. (Color online) (a) The complex refractive index for a dense 100 nm silver film as a function of wavelength extracted with ellipsometry, solid line, Drude-Lorentz fit, dash-dotted line; (b) the real and imaginary parts of the effective refractive index for the Ag-Al_2O_3 nanostructures with different volume fraction of Ag: $f=0.1, 0.15, 0.2$.

$$\varepsilon(\omega) = \varepsilon_0 - \frac{\omega_p^2}{\omega^2+i\omega\gamma} - \sum_{j=1}^{3}\frac{\Delta\varepsilon_j\Omega_j^2}{\omega^2-\Omega_j^2+i\omega\Gamma_j}. \tag{8}$$

A very good agreement between the extracted experimental dependence of $n_{exp}=n+ik$ and the analytical formula (8) was obtained for the following parameters: $\varepsilon_0=4.5$; $\Delta\varepsilon_j=(1.0, 1.1)$; $\hbar\omega_p=9.0$ eV $\hbar\gamma=0.07$ eV; $\hbar\Omega_j=(4.5, 5.7)$ eV; $\hbar\Gamma_j=(1.2, 2.7)$ eV, where $j=1, 2$. Figure 6(a) shows the real and imaginary part of the refractive index of Ag particles used in our calculation as a function of wavelength. The optical constants of an Al_2O_3 film have been parameterized by the Cauchy function. To find Cauchy coefficients we again carried out spectroscopic ellipsometry measurements of pure Al_2O_3 film. The refractive index of Al_2O_3 films shows low dispersion with values of $n_d=1.725-0.02$ throughout the visible and near IR spectral range.

Using Eqs. (2)–(8), we simultaneously calculated the effective refractive index (see Fig. 6), optical transmission and reflection spectra [Fig. 5(b)]. The reflectance spectra at normal incidence were calculated with the help of the Fresnel equations for a two layer system: a uniform layer of silver nanospheres in Al_2O_3 matrix (effective medium) and a thick glass substrate (1 mm). The thickness of the effective layer has been chosen to be higher than diameter of silver nanoparticles ($h\sim160$ nm). The main goal of the calculations

was to find conditions at which the reflectance R and transmittance T are minimal. Figure 5(b) shows the calculated reflection and transmission spectra of the Ag-Al_2O_3 nanostructures for small filling factor, f, ranging from 0.1 to 0.2 and average diameter of particles about $D \approx 120$ nm. The reflectance at normal incidence was calculated using the effective index of refraction and including log-normal particle-size distributions. Using the Kirchhoff's rule (the sum of the transmittance $T(\lambda)$, reflectance $R(\lambda)$, and absorbance $A(\lambda)$ should equal 1 in the absence of diffuse scattering), we concluded that the coefficient of absorption for the studied nanostructure can be higher 95% in the wavelength range of 240–800 nm, see Fig. 5(b). Thus the light absorption was optimized for normal light incidence with respect to three parameters, f, D, and h. Numerical optimizations for $h = 150-160$ nm suggested that the lowest reflected and transmitted intensities (of about 2–5 %) are achieved for the values of the $f=0.1-0.2$, $D=100-120$ nm. The calculated dependences demonstrate that the studied composites can be optimized to yield absorption of light at the level above 95% for unpolarized light in spectral region 240–850 nm.

The calculated complex refractive index of Ag-Al_2O_3 composite films using the EMA approach is shown in Fig. 6(b). We compared the values of $n_{eff}+ik_{eff}$ for the Ag-Al_2O_3 nanostructures of different volume fraction f. Figure 6(b) shows that $n_{eff}+ik_{eff}$ depends more strongly on f at the wavelength region 600–1000 nm. We also see that the real part of the refractive index n_{eff} increases with the increase in wavelength. The values of n_{eff} ranged from 1.2 to 1.7; they are much higher than that of bulk Ag [e.g., $n=0.04$, $\lambda = 825$ nm (Ref. 14)]. The imaginary part of refractive index, k_{eff}, increases with increasing volume concentration of Ag particles, f. One pronounced extinction peak appeared in all k_{eff} curves, see Fig. 6(b). This peak can be associated with excitation of localized surface plasmons in silver particles. This absorption peak is redshifted when the volume concentration of silver particles is increased. The values of k_{eff} are small, except for those in the surface plasmon resonance extinction region, indicating that these nanostructures selectively absorbed and scattered incident light at specific wavelength bands. The silver nanoparticles embedded in Al_2O_3 matrix exhibit a spectrally broad dipolar resonance due to distribution particles in sizes. Note that the n_{eff} curves are highly affected by the k_{eff} dependences. In the weakly absorbing region (values of k_{eff} are small for $\lambda < 500$ nm) the refractive index n_{eff} remained constant ($1.2 < n_{eff} < 1.3$) for the various samples. In the absorbing region ($k_{eff} > 0.2$) the refractive index curves exhibited abnormal dispersion behaviors. We can conclude that spectral region between 600 and 1000 nm is highly sensitive to the extremely small changes in the effective optical constants for plasmonlike nanostructures.

Effective-medium calculations suggest that a high level of light absorption can be realized in thin artificial layers made of metal nanoparticles embedded in dielectric matrix. The size of the metal nanoparticles plays an important role in the observed effects. Larger nanoparticles have larger polarizabilities and provide higher absorption efficiencies. It is worth noting that suggested nanostructured films are relatively simple and cheap to fabricate over large areas. Below we compare our experimental results with these theoretical predictions.

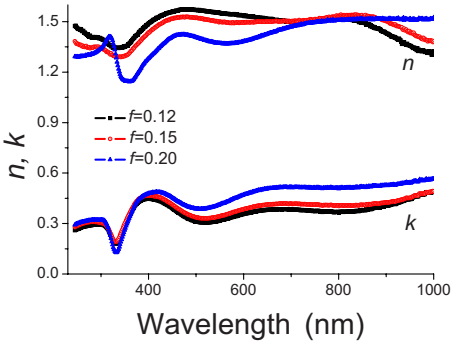

FIG. 7. (Color online) Experimental approbation of the effective-medium theory. The complex refractive index for the Ag-Al_2O_3 nanostructures as a function of wavelength extracted with ellipsometric measurements based on model of effective layer for different volume fraction of Ag: $f=0.12, 0.15, 0.2$.

V. DISCUSSION

Measured wavelength dependences of the $R_P(\lambda)$ and $T_P(\lambda)$ coefficients [Figs. 3(a) and 3(b)] are in good agreement with the theoretical data [Figs. 5(a) and 5(b)]. In particular, the position of the maxima ($\lambda \sim 350$ nm) in $R_P(\lambda)$ spectral dependences is nicely reproduced, and the reflection and transmission spectra show small variations with wavelengths and incident angles and keep the level at 2–5 %. Broad peaks in transmission occur at $\lambda \sim 320$ nm for all angles of incidence (Fig. 2). An absorption peak at $\lambda \sim 320$ nm can be assigned to the interband transitions of d electrons in silver particles modified by the presence of dielectric host {i.e., at the plasmon resonance condition $\mathrm{Re}[\varepsilon(\mathrm{Ag})] = -2\varepsilon_d(Al_2O_3)$}. The real part of the silver dielectric constant significantly increases at these wavelengths (Fig. 6).

In order to understand the role of silver nanoparticles in the enhancement of light absorption we have compared the experimental and theoretical effective dielectric functions. The effective complex index of refraction $n_{eff}+ik_{eff}$ was directly extracted from the measured ellipsometric parameters $\psi(\lambda)$ and $\Delta(\lambda)$. The result is shown in Fig. 7 as a function of filling factor, f. It is easy to see that k_{eff} increases with increasing filling factor f while the n_{eff} decreases in the region 400–800 nm. We notice that n_{eff} is ranged between 1.2 and 1.7 over the entire visible and near IR region, implying mostly dielectric response. The dependences of n_{eff} and k_{eff} display three broad peaks. The extinction peaks, k_{eff}, are blueshifted in comparison to those in the n_{eff} curves. Additionally, the effective refractive index $n_{eff}+ik_{eff}$ inverts the main tendency of the refractive index of noble metal, Ag. The values of the complex refractive index of Ag, which are typical for all noble metals, are next: smallness of the real part n (less than 1) and a large of the imaginary part $k \geq 1$ in visible and near-IR spectral regions. Obtained values n_{eff} and k_{eff} are in good agreement with values of $n_{eff}^{\perp} \approx 1.6$ and $k_{eff}^{\perp} \approx 0.3$ for the effective EMA constants obtained for gold

nanostripe structures in our recent work (Ref. 10) that described the plasmonic blackbody in the wavelength range 240–520 nm. There are some difference between extracted and calculated values of k_{eff} which arises due to the presence of trapped light modes. These modes effectively increase the path of light propagation in the metamaterial and therefore increase the sample thickness in the EMA approach. It is also worth noting that the effective optical constants extracted for Ag-Al_2O_3 structures in the wavelength range of "blackbody" behavior (400–850 nm), are close to the values of the effective constants which would guarantee the maximal absorption in accordance with the Fresnel coefficients shown in Figs. 5 and 6.

The experimental results (Fig. 7) are in a good agreement with the simulated functions of $n_{eff}+ik_{eff}$ (Fig. 6) for wavelengths 500–850 nm. A poorer agreement between experimental and modeled refractive index was obtained at longer and shorter wavelengths. We explain this by the presence of the guided light modes propagating along the film and arising due to total internal reflection [Fig. 1(d)]. The deviation of the theory and experiment at short wavelengths can be due to the interband transitions in silver nanoparticles. Introduced Drude-Lorentz approximation is not ideal for description of optical properties of silver nanoparticles. In bulk silver the interband transition from occupied d states to unoccupied p and s states above Fermi level appear at 4 eV (310 nm) and 3.5 eV (350 nm),[14] respectively. For silver nanostructures such electron transitions from d states to p and s states become allowed at frequencies below 3.5 eV (350 nm) and depend on nanostructure geometry. Additionally, the quantitative differences between experimental (Fig. 7) and theoretical (Fig. 6) data at short wavelengths could arise because of the presence of nonstoichiometric AgO_x oxides and nonspherical Ag nanoparticles. We found that the Fresnel model with an additional roughness layer with voids ($\sim$3–5 nm thick) on top of Ag-Al_2O_3 film resulted in a better fit to experimental ellipsometric functions $\psi(\lambda)$ and $\Delta(\lambda)$. This agrees with the conclusion of Aspnes *et al.*[20] who stressed that noble film grown at slightly different conditions could have considerably different optical constants n_{eff} and k_{eff} above the interband transitions due to contribution of small defects such as voids.

It is worth noting that the spectral behavior of the calculated effective refractive index reflects the main features in $R_p(\lambda)$ and $T_p(\lambda)$. The occurrence of broad peaks in the $R_p(\lambda)$ and $R_s(\lambda)$ spectra (Figs. 3 and 4) is correlated with main features of effective refractive index $n_{eff}+ik_{eff}$ which describes the collective optical properties of the nanostructures. First, the energy position of broad peak at 300–500 nm in $R_p(\lambda)$, $R_s(\lambda)$, and $A_p(\lambda)$ spectra (Figs. 3 and 4) correlates with appearance of the maxima in n_{eff}. Second, the broad maxima in the region of 650–800 nm in the n_{eff} and k_{eff} spectra look like as the features in $R_p(\lambda)$ and $A_p(\lambda)$ dependences for large angles of incidence. These features in $R_p(\lambda)$ and $A_p(\lambda)$ are shifted toward the larger wavelengths in comparison to ones in the n_{eff} and k_{eff}. Physically, the origin of these broad maxima can come from excitation of localized plasmons in isolated silver particles. Due to the negative real part of the dielectric constant of silver, $\mathrm{Re}[\varepsilon(\omega)]$, incident light excites localized plasmon resonances, which shift in near IR region (700–800 nm) for particles of large sizes ($D \geq 100$ nm).[21–23] These resonances can occur at discrete frequencies and are strongly localized in skin surface layer of large particles. Due to dipole-dipole interaction between ensemble of particles and strong coupling between localized plasmon these resonances tend to broadening and producing tight bound bands. Existence of such plasmon bands is a good condition for creating plasmonic structures with blackbody behaviors.[10] An important part of the interaction of light with plasmon-active nanostructures is the trapping and conversion of the incident radiation which can be used to enhance the efficiency of solar cells and photodetectors.[24,25] In this research it was also experimentally shown the strong correlation between macroscopic optical characteristics as a reflection and transmission and spectral dependencies of the effective optical constants. Due to this connection it is possible to determine the effective complex refractive index $n_{eff}+ik_{eff}$ *in situ* using ellipsometry and obtain desire values of absorption spectra. Such control of the optical properties can be very important during performance of large area of high-efficiency solar cells.

VI. CONCLUSIONS

We showed that the optical properties of Ag-Al_2O_3 nanostructures can be tuned by adjusting the size and concentration of silver nanoparticles in Al_2O_3 matrix and thickness of layer. The main properties of these systems are studied within the frame of the Mie theory of particle dipole polarizability and macroscopic behaviors described by the Maxwell-Garnett-type effective-medium theory. We demonstrated that for such structures the level of light absorption more than 95% can be achieved in a wavelength range of 240–850 nm for the large range of the incident angles ($0°-70°$) and for the light with electric-field vector parallel to incident plane (p-polarized light). Absorption higher than 90% for both polarizations (p- and s-polarized or unpolarized light) in a range of angle of incidence equal to ($0°-45°$) was revealed. It was shown that experimentally observed dependence of the absorption in nanostructure thin film can be explained on the basis of EMA theory with introduction of effective complex refractive index and using Fresnel reflection and transmission coefficients for thin film on top of glass substrate. We found that the effective optical constants $n_{eff}+ik_{eff}$ of silver nanostructures determined through spectroscopic ellipsometry are highly sensitive to changes in the particle sizes, particle covering, and thickness of layer. It is therefore important to monitor the refractive index of fabricated plasmonic metamaterial *in situ* with the aim to achieve desired absorption characteristics.

The proposed method for fabrication of thin-film blackbody inexpensive metamaterials (which strongly absorb light in broad spectral range as well as a wide interval of angles of incidence) could be applied to other metallic nanoparticles (Cu, Au, and Pd) that have a large reflectivity for bulklike states and for Si nanostructures or Si nanoparticles covered by Ag shell. The light incident on these structures can excite localized plasmon resonances, inducing polarization currents in the individual particles and transfer a significant portion of

energy into surface modes. Metal nanostructured thin-film metamaterials can find application for subwavelength energy accumulation in photodetectors, photoconverters, and a new generation of low-cost high-efficiency solar cells.

ACKNOWLEDGMENT

This work has been supported by EPSRC under Grant No. EP/E01111X/1.

[1] F. Z. Yang, J. R. Sambles, and G. W. Bradberry, Phys. Rev. B **44**, 5855 (1991).
[2] K. R. Catchpole and A. Polman, Opt. Express **16**, 21793 (2008).
[3] H. R. Stuart and D. G. Hall, Appl. Phys. Lett. **73**, 3815 (1998).
[4] K. R. Catchpole and A. Polman, Appl. Phys. Lett. **93**, 191113 (2008).
[5] A. N. Grigorenko, A. K. Geim, H. F. Gleeson, Y. Zhang, A. A. Firsov, I. Y. Khrushchev, and J. Petrovic, Nature (London) **438**, 335 (2005).
[6] W.-C. Tan, J. R. Sambles, and T. W. Preist, Phys. Rev. B **61**, 13177 (2000).
[7] M. Kreiter, J. Oster, R. Sambles, S. Herminghaus, S. Mittler-Neher, and W. Knoll, Opt. Commun. **168**, 117 (1999).
[8] E. Popov, D. Maystre, R. C. McPhedran, M. Neviere, M. C. Hutley, and G. H. Derrick, Opt. Express **16**, 6146 (2008).
[9] E. Popov, S. Enoch, and N. Bonod, Opt. Express **17**, 6770 (2009).
[10] V. G. Kravets, F. Schedin, and A. N. Grigorenko, Phys. Rev. B **78**, 205405 (2008).
[11] J. C. Maxwell-Garnett, Philos. Trans. R. Soc. London, Ser. A **203**, 385 (1904).
[12] F. J. García-Vidal, J. M. Pitarke, and J. B. Pendry, Phys. Rev. Lett. **78**, 4289 (1997).
[13] R. M. A. Azzam and N. M. Bashara, *Ellipsometry and Polarized Light* (North-Holland Press, Amsterdam, 1987).
[14] E. D. Palik, *Handbook of Optical Constants of Solids* (Academic, San Diego, 1998).
[15] C. F. Bohren and D. R. Huffman, *Absorption and Scattering of Light by Small Particles* (Wiley, New York, 1983).
[16] E. Yablonovitch, J. Opt. Soc. Am. **72**, 899 (1982); E. Yablonovitch and G. D. Cody, IEEE Trans. Electron Devices **ED–29**, 300 (1982).
[17] W. T. Doyle, Phys. Rev. B **39**, 9852 (1989).
[18] V. A. Markel, J. Phys. B **38**, L115 (2005).
[19] R. Ruppin, Opt. Commun. **182**, 273 (2000).
[20] D. E. Aspnes, E. Kinsbron, and D. D. Bacon, Phys. Rev. B **21**, 3290 (1980).
[21] A. V. Zayats and I. I. Smolyaninov, J. Opt. A, Pure Appl. Opt. **5**, S16 (2003).
[22] F. J. García de Abajo, Rev. Mod. Phys. **79**, 1267 (2007).
[23] V. G. Kravets, F. Schedin, and A. N. Grigorenko, Phys. Rev. Lett. **101**, 087403 (2008).
[24] L. Eurenius, C. Hagglund, E. Olsson, B. Kasemo, and D. Chakarov, Nat. Photonics **2**, 360 (2008).
[25] H. R. Stuart and D. G. Hall, Phys. Rev. Lett. **80**, 5663 (1998).